Cryoconcentration of Flavonoid Extract for Enhanced Biophotovoltaics and pH Sensitive Thin Films

A. Demirbas
Agricultural and Biological Engineering, Institute of Food and Agricultural Sciences, University of Florida, Gainesville, FL

K. Groszman
Department of Computational and Applied Mathematics, Rice University, Houston, TX

M. Pazmiño-Hernandez
Agricultural and Biological Engineering, Institute of Food and Agricultural Sciences, University of Florida, Gainesville, FL

D. C. Vanegas
Food Engineering Department, Universidad del Valle, Cali Colombia

B. Welt
Agricultural and Biological Engineering, Institute of Food and Agricultural Sciences, University of Florida, Gainesville, FL

J. A. Hondred
Mechanical Engineering Department, Iowa State University, Iowa City, IA

N. T. Garland
Mechanical Engineering Department, Iowa State University, Iowa City, IA

J. C. Claussen
Mechanical Engineering Department, Iowa State University, Iowa City, IA

E. S. McLamore
Agricultural and Biological Engineering, Institute of Food and Agricultural Sciences, University of Florida, Gainesville, FL

DOI 10.1002/btpr.2557
Published online October 4, 2017 in Wiley Online Library (wileyonlinelibrary.com)

Flavonoids are important value added products for dye sensitized solar cells biosensors, functional foods, medicinal supplements, nanomaterial synthesis, and other applications. Brassica oleracea *contains high levels of anthocyanins in leaf sap vacuoles, and there are many viable extraction techniques that vary in terms of simplicity, environmental impact, cost, and extract photochemical/electrochemical properties. The efficiency of value added biotechnologies from flavonoid is a function of anthocyanin activity/concentration and molecule stability (i.e., ability to retain molecular resonance under a wide range of conditions). In this paper, we show that block cryoconcentration and partial thawing of anthocyanin from* B. oleracea *is a green, facile, and highly efficient technique that does not require any special equipment or protocols for producing enhanced value added products. Cryoconcentration increased anthocyanin activity and total phenol content approximately 10 times compared with common extraction techniques. Cryoconcentrated extract had enhanced electrochemical properties (higher oxidation potential), improved chroma, and higher UV absorbance than extract produced with other methods for a pH range of 2–12, with minimal effect on the diffusion coefficient of the extract. As a proof of concept for energy harvesting and sensor applications, dye sensitized solar cells and pH-sensitive thin films were prepared and tested. These devices were comparable with other recently published biotechnologies in terms of efficacy, but did not require expensive/environmentally detrimental extraction or concentration methods. This low cost, biorenewable, and simple method can be used for development of a variety of value added products.* © 2017 American Institute of Chemical Engineers *Biotechnol. Prog.*, 34:206–217, 2018
Keywords: anthocyanin, cryoconcentration, dye sensitized solar cell, pH sensitive thin film

Introduction

In plants, flavins are involved in photoprotection and phototransduction,[1] nitrogen translocation,[2] and pollinator attraction.[3] Flavins include carotenoids (liposoluble) and anthocyanins

Additional Supporting Information may be found in the online version of this article.

Correspondence concerning this article should be addressed to E. S. McLamore at emclamor@ufl.edu

(water soluble), each class having a range of antioxidant and photochemical properties.[4,5] Plants that are rich in anthocyanins include blueberries, raspberries, concord grapes, and red cabbage.[6] Anthocyanin extracts are used as food additives,[7,8] medicinal supplements,[9,10] molecular templates for nanomaterial synthesis,[11,12] various cosmetic applications,[13] dye-sensitized solar cells,[14,15] and as biodetectors.[16,17] Due to the diverse applications of anthocyanins, research on the development of this value added agricultural product has increased in the last decade.[18–20]

The general photochemistry of anthocyanins is well known.[21,22] Due to the aromatic cyclic arrangement, anthocyanins absorb low energy radiation, which varies depending on pH as a function of molecular resonance. Some anthocyanins have demonstrated fluorescence with emission near 600–630 nm,[23,24] while some inhibit fluorescence of bioconjugates such as DNA–propidium iodide.[25] Red cabbage (*Brassica oleracea* L. var. *capitata)* can have up to 36 different anthocyanins, each of which vary in terms of physicochemical properties and stability.[26] *B. oleracea* anthocyanins are primarily composed of cyanidin or peonidin based aglycones, although pelargonidin has been reported as well. Most *B. oleracea* anthocyanins are mono or di-acylated anthocyanins, with acid moieties consisting of sinapic, ferulic, caffeic and *p*-coumaric acids.

Anthocyanins from *B. oleracea* are encased in leaf sap vacuoles and can be extracted using high pressure extraction,[27] microwave irradiation,[28] supercritical fluid extraction,[29] Soxhlet/solvent extraction,[27] adsorbent purification,[14] ultrasonic treatment,[30] or pulsed electric field processing,[31] among other techniques. The antioxidant and optical properties of extracts vary widely for these methods, even for the same species and harvest season.[32] The efficacy of many biotechnologies that utilize anthocyanins as a working component of the device (e.g., solar cells, sensors, functional foods) are dependent on the total concentration and chemicophysical properties of the extract, where native physiological structures are desired (pH = 7, low salinity, absence of solvents). Methods for increasing extract yield include passive cryoconcentration,[33–35] vacuum-assisted cryoconcentration,[36] centrifugal cryoconcentration,[37] falling film freeze concentration,[38] and nanofiltration.[39] For development of new technologies such as sensors/biosolar cells, many of these concentration methods are cost prohibitive, as they require expensive consumables, high pressure, large centrifuges, or other equipment. This high cost often impedes translation to the industrial market, creating a bottleneck of biotechnologies. Among the concentration methods listed here, cryoconcentration with passive thawing and gravity separation is the most attractive green method, as it can be conducted at physiological pH in the absence of solvents. This is a critical feature for manufacturing of sensors/biosolar cells at any appreciable scale. Further, the technique uses commonly available equipment, and thus capital costs are low for implementation.

In this paper, we conduct a comparative study of facile anthocyanin extraction techniques including solvent extraction, microwave assisted extraction, and conductive heating. We compare three parameters for variations of each technique: (i) total anthocyanin content, (ii) antioxidant activity, and (iii) total polyphenol content. To improve yield, block cryoconcentration followed by passive partial thawing was used and then anthocyanin content, antioxidant activity as well as total phenol content were monitored over time. Next, the most efficient extraction/concentration method was analyzed using standard electrochemical and photochemical techniques. Finally, we demonstrate potential applications by developing and testing a dye sensitized solar cell and a pH sensitive thin film using cabbage extract.

Methodology

Reagents and chemicals

Red cabbage (*Brassica oleracea* var. capitata, f, rubra) was purchased from an organic market in Gainesville, FL during the spring. Methanol (CH_3OH), acetic acid (CH_3COOH),citric acid ($C_6H_5O_7^{3-}$), disodium phosphate (Na_2HPO_4), potassium ferrocyanide ($KFeCN_6$), lithium perchlorate ($ClLiO_4$), sodium carbonate (Na_2CO_3), potassium nitrate (KNO_3) potassium chloride (KCl), sodium hydroxide (NaOH), hydrochloric acid (HCl), sodium acetate (CH_3COONa), sodium bicarbonate ($NaHCO_3$), sodium carbonate (Na_2CO_3), potassium iodide, Folin–Ciocalteu reagent, and biological buffers (MES, BES, TRIZMA, AMPSO, CAPS, and CABS) were purchased from Sigma-Aldrich (St. Louis, MO).DPPH (1,1-diphenyl-2-picrylhydrazyl) was purchased from Fisher Scientific (Atlanta, GA). Trolox (6-hydroxy-2,5,7,8-tetramethylchroman-2-carboxylic acid) was purchased from Alexis (Axxora, Switzerland). Platinum wire (0.3 mm diameter) was purchased from Alfa Aesar (Ward Hill, MD), and working electrodes (Pt/Ir and glassy carbon) were purchased from Bioanalytical Systems (West Lafayette, IN). Titanium dioxide (TiO_2) nanoparticle paste (Nanoxide-T, colloidal anatase with particle size of 13 nm) was obtained from Solaronix (Aubonne, Switzerland).

Preparation of extract

B. oleracea leaves were pulled from the stem, the stem was discarded, and leaves were chopped into 1 cm^2 pieces using an autoclaved knife. Any leaves that did not contain purple pigment were discarded. Four different methods were used for extraction, including (i) solvent extraction, (ii) microwave assisted extraction, (iii) conduction (boiling), and (iv) conduction with cryoconcentration. For solvent and microwave extraction, aliquots of chopped leaves (100 g) were added to either 100 mL methanol at varying dilutions, or 100 mL DI water with 10% acetic acid, respectively. For microwave-assisted extraction, the power was 1000 W and treatment times of 0, 30, 45, 60, 90, 120, 240, or 480 s were used (average final temperature for all samples was 95 ± 6°C). The sample was placed in the center of the microwave for all relevant experiments. For conduction-based extraction, 100 g of fresh chopped leaves were added to 100 mL of DI water and samples were heated at different temperatures (25, 45, 60, 80, or 100°C) for either 30 min or 1 h.

For cryoconcentration, samples were transferred to a plastic container, sealed, and stored at −80°C for at least 2 h immediately after extraction. No pretreatment was used for the freeze concentrated extract, and no agitation was used during the freezing process (known as "block concentration"). After block freezing, samples were stored at 20°C and the extract at the bottom of the plastic container (a viscous purple syrup) was collected after 5 min, 1, 5, and 24 h, and analyzed immediately as noted (see highlight image). All aqueous extracts were vacuum filtered using a 0.45 μm

cellulose acetate filter Whatman (Kent, WA) prior to analysis.

Total anthocyanin content

Total anthocyanin content was measured using the differential pH method by Lee et al.,[40] which is a rapid and simple spectrophotometric method based on the anthocyanin structural transformation that occurs with a change in pigment color at pH 1.0 versus pH 4.5. Two buffer systems were used including potassium chloride buffer (0.025M, pH = 1.0) and sodium acetate buffer (0.4M, pH = 4.5). An aliquot of the cabbage extract (1.0 mL) was placed in a 20 mL volumetric flask, diluted to volume with pH 1.0 buffer or pH 4.5 buffer, and mixed. Both solutions were incubated at room temperature for 20 min. Prepared solutions were then measured with a UV/VIS spectrophotometer (Beckman Coulter DU-640 spectrophotometer, Beckman Instruments, CA, USA) at 510 and 700 nm. Anthocyanin was calculated according to Eq. 1 and expressed as mg of cyanidin-3-glucoside (c3g) per gram of cabbage:

$$\text{Antho} = \frac{A * \text{MW} * \text{DF}}{\varepsilon * I} \quad (1)$$

where

Antho = anthocyanin concentration (mg-c3g/L),

A = differential absorbance = $(A_{510} - A_{700})$ at pH1.0 – $(A_{510} - A_{700})$ at pH4.5,

A_{510} = absorbance at λ = 510 nm (arb. units),

A_{700} = absorbance at λ = 720 nm (arb. units),

MW = molecular weight (611 g/mol for c3g),

DF = dilution factor,

I = path length (cm), and

ε = molar extinction coefficient for c3g (30,175 L × mol^{-1} × cm^{-1}).

Antioxidant activity

Antioxidant activity was evaluated using a modified version of the Trolox equivalent antioxidant capacity (TEAC) assay.[41] Stock solutions were prepared by dissolving 24 mg DPPH with 100 mL methanol and then storing at −20°C when not in use. The working solution was obtained by mixing 10 mL stock solution with 45 mL methanol to obtain an absorbance of 1.1 ± 0.02 U at 515 nm for a blank sample (methanol). Cabbage extract (100 μL) was reacted with 3900 μL of the DPPH solution for 60 min in the dark at room temperature. Meanwhile, a 100 μL aliquot of Trolox solution with respective concentrations of 100, 200, 400, 600, 800, or 1000 μM was added to 3.9 mL DPPH working solution for generating the standard curve. Then, absorbance was recorded at 515 nm and results were expressed in molarity of Trolox equivalent per mass of wet extract.

Total polyphenol content

Total phenolic content was determined using a modified version of the Folin–Ciocalteu assay based on Stanković[42] and Piljac et al.[43] Gallic acid (GA) was used as the standard and all data was expressed as mass of GA equivalents per mass of dry defatted matter (mg-GAE/g-DM) based on GA calibration curves. Samples and prepared standards were incubated for 30 min in a 40°C water bath, and absorbance was measured at λ = 760 nm using a spectrometer. Aliquots of 5 mL samples contained 2% (w/w) sample, 5% (w/w) Folin–Ciocalteu reagent, 15% (w/w) Na_2CO_3, and 78% (w/w) DI water.

Electrochemistry

To determine the diffusion properties of the extract (an estimate of molecular weight) as well as the general anthocyanin content, electrochemical analysis of extract was carried out based on published methods.[44–46] For all analysis, cyclic voltammetry (CV) and linear sweep voltammetry (LSV) were carried out in buffer at 20°C. Bulk pH in the electrochemical cell was monitored with a standard potentiometric glass pH probe (Orion 9109WL, Thermo Scientific) during all CV and LSV experiments. For studying the effect(s) of pH, extract (1 mL) was added to a 10 mL electrochemical cell with buffers at various pKa, including: (i) 79.5 mM citric acid with 20.6 mM Na_2HPO_4 (pK_a = 3.0), ii) 61.5 mM citric acid with 38.6 mM Na_2HPO_4 (pKa = 4.0), iii) 48.5 mM citric acid with 51.5 mM Na_2HPO_4 (pKa = 5.0), iv) MES (pKa = 6.1), v) MOPS (pKa = 7.2), vi) TRIZMA (pKa = 8.1), vii) AMPSO (pKa = 8.9), viii) CAPS (pKa = 10.4), and ix) 90 mM Na_2CO_3 with 10 mM $NaHCO_3$.

All experiments used a three-electrode cell stand (Bioanalytical Systems, West Lafayette, IN) with a glassy carbon or Pt/Ir working electrode, a 1 mm platinum wire as counter electrode, and a Ag/AgCl reference electrode as previously described.[47–49]All CV analyses were performed with a Pt/Ir electrode in potassium ferrocyanide (4 mM) at a switching potential of 600 mV with a five second quiet time at scan rates of 25–500 mV s^{-1} as noted. LSV was performed with a glassy carbon electrode between 0 and 800 mV at a scan rate of 5 mV s^{-1}, with lithium perchlorate (0.1 mM) as the supporting electrolyte. The Randles–Sevcik theorem was used to calculate the diffusion coefficient for a given total concentration based on Ref. (50).

$$i_p = 2.69 \times 10^5 * n^{3/2} * A * D^{1/2} * C * v^{1/2}$$

where

i_p = oxidative/reductive peak current (A),

n = number of electrons transferred in redox reaction,

D = diffusion coefficient (cm^2 s^{-1}),

C = total anthocyanin concentration (M),

A = electroactive surface area of working electrode (0.02 cm^2), and

V = scan rate (V s^{-1}).

Photochemistry

Photochemistry was performed using an Ocean Optics fiber optic UV–VIS spectrometer with fiber optic accessory from 250 to 850 nm (Ocean Optics, Dunedin, FL). A P-400-2-UV–VIS fiber optic cable (Ocean Optics) was used where noted. Where noted, the fiber was positioned near the thin film using a precision linear micromanipulator stage (2 μm resolution) with custom fiber housing (Newport Corporation, San Francisco CA). Extract (1 mL) was added to a cuvette with 3 mL of buffer at various pKa values as described in the previous section. Samples were added to sterile cuvettes, inverted to mix, and then absorbance was measured (relative to a control sample of DI water). Where noted, thin films

were measured using a 100 μm single mode silicone-coated UV–VIS fiber and a custom 3D printed film analysis setup. A boxcar width of 15 and an integration time of 100 ms was used for all samples. For analyzing color of each sample, the CIE LAB system was used, which is an international standard defined by the Commission Internationale de l'Eclairage using a chromaticity diagram. In this system, L = luminance, A = red green chromaticity, and B = blue-yellow chromaticity.

Proof of principle applications

There are a variety of applications for anthocyanin derived from cabbage beyond food additives. To show two specific applications, flavonoid-sensitized solar cells (i.e., Grätzel cells) were prepared based on the methods by Kumara et al.[51] (see Supporting Information Figure S1 for schematic, energy diagram, and typical *I–E* curve). Manufacture of these solar cells is described in detail by Kumara et al. Briefly, photo electrodes were prepared by coating precleaned fluorine doped tin oxide (FTO) glass (50 mm × 50 mm, 1.1 mm thick, 7 Ω sheet resistance) with TiO_2 nanoparticle paste using the doctor blade method (40–50 μm film thickness). Electrodes (1 cm × 1 cm) were preheated to 50°C for 20 min and then sintered at 450°C for 30 min. Photoelectrodes were then immersed into extract for 20 min at room temperature, rinsed in ethanol, and then air dried at room temperature for 30 min. Solar cells were assembled by coupling the flavonoid-sensitized FTO electrode (anode) with a carbon-coated FTO glass slide (cathode) and clamping the ends. The electrolyte (0.5M potassium iodide) was added by drop casting 50 μL onto each edge of the glass electrode interface, and cells were allowed to stabilize at room temperature in the presence of 1000 W/m^2 white light for 20 min. Based on *I–E* curves, the short circuit current density (J_{sc}), open circuit voltage (V_{oc}), maximum power output (P_{max}), voltage at max power (V_{mp}), current density at max power (J_{mp}), form factor (FF), and solar conversion efficiency (η) were calculated using the methods reported by Hug et al.[52]

Inkjet printing of the extract closely followed our similar procedures for printing graphene inks.[53–55] For preparing inkjet-printed thin film biodetectors, aliquots (3 mL) of extract were filtered through a 0.45 μm. Polytetrafluoroethylene (PTFE) syringe filter and then loaded into an inkjet printer cartridge (1.5 mL max. fill) and then printed through inkjet printer (Fujifilm Dimatix DMP-2850) using a piezoelectric driven nozzle with a 10 pL nominal drop volume. The substrate holder (vacuum plate) was maintained at 50°C to ensure uniform, rapid drying of the printed ink. Extract was inkjet printed with a 20 μm drop spacing and 25 passes. These printer settings permit an even printing of the extract without holes/gaps in the film and without material pooling effects at the edges. The printed line morphology resulting from the drop spacing and the working temperature control edge effects (known as the coffee ring effect). Our previous work shows that average film thickness is between 3 and 5 μm, classifying this structure as a thin film.[53–55] A circular array was designed using computer-aided design (CAD software) and inkjet printed. For unbuffered calibration tests, pH was adjusted with 3M HCl or 2M NaOH, and then 5 μL aliquots were drop cast onto the pH sensitive film. For buffered calibration tests, 10 mM stock solutions of buffer (as described previously) and drop cast as described above.

For testing pH sensitive films, water samples from a local lake, and soil slurry samples from various soil types were prepared. Water samples from Lake Alice conservation area at the University of Florida (Gainesville, FL) were acquired in November, 2016. The location includes 130 acres of protected area, with an 82 acre open water system that has inputs from stormwater runoff, interstorm discharges, irrigation water, and direct rainfall. Samples were collected near the southeast storm sewer drainage pipe at noon, and analyzed on site immediately. Soil samples were taken from two vegetable garden sites (Gainesville, FL). One plot contained oak–saw palmetto scrub (Alaquods) that had compost (10% w/w) applied weekly for the past 5 years (noted as organic soil). The second sample site consisted of a garden that was prepared with commercial soil (Miracle Gro©) that contained a mixture of perlite (99.44%), ammonia nitrogen (0.035%), nitrate nitrogen (0.035%), phosphorous pentoxide–P_2O_5 (0.07%), soluble potash–K_2O (0.07%), and proprietary wetting agents (0.07%). For tests, a 1:2 (soil:electrolyte) soil slurry was prepared by mixing 10 g of soil sample with 20 mL of 10 mM $CaCl_2$. The soil slurry was subsequently stirred vigorously and allowed to settle for 15 min. This measurement avoids bias by varying salt concentrations among the soils, which is the official method adopted by the Association of Official Analytical Chemists.[56] The liquid extract was measured by either immersing the pH electrode in the sample vial or drop casting the slurry based on Miller and Kissel.[56] After drop casting the sample on the pH-sensitive film, the fiber optic probe was positioned 1 mm from the surface using the micromanipulator, and a measurement taken.

Statistics and data analysis

Analysis of variance (ANOVA model I) was performed to determine whether any effects in the optical properties of the films are statistically significant ($\alpha = 0.05$). Where relevant, error bars represent the standard deviation of the arithmetic mean for the random experimental design.

RESULTS AND DISCUSSION

Extract anthocyanin and phenolic content

Figure 1 shows the average anthocyanin content, antioxidant activity, and total phenol content for extractions using various solvent extraction (100% methanol), microwave irradiation (8 min) and boiling methods. For variations of each method see the Supporting Information section (Supporting Information Figures S2–S4). The average anthocyanin content for solvent extraction at room temperature, microwave irradiation, and conduction for 1 h were not significantly different ($P = 0.15$, $\alpha = 0.05$). The anthocyanin content (Figure 1a) for solvent (methanol) extraction, microwave (MW) (120 s), MW + acetic acid (10%), and boiling were not significantly different. Microwave irradiation for 8 min or boiling for 60 min increased anthocyanin content by at least 35% compared with the other methods (MW for 8 min and boiling for 1 h were not statistically different ($P = 0.001$, $\alpha = 0.05$). Antioxidant activity (Figure 1b) and total phenol content (Figure 1c) were at least 40% higher for 60 min of boiling compared with solvent extraction, although this was not statistically different than boiling for 30 min, MW (8 min) + AA (10%), or MW (8 min). Among all extraction methods, the highest absorption ($\lambda = 435$ nm) was for

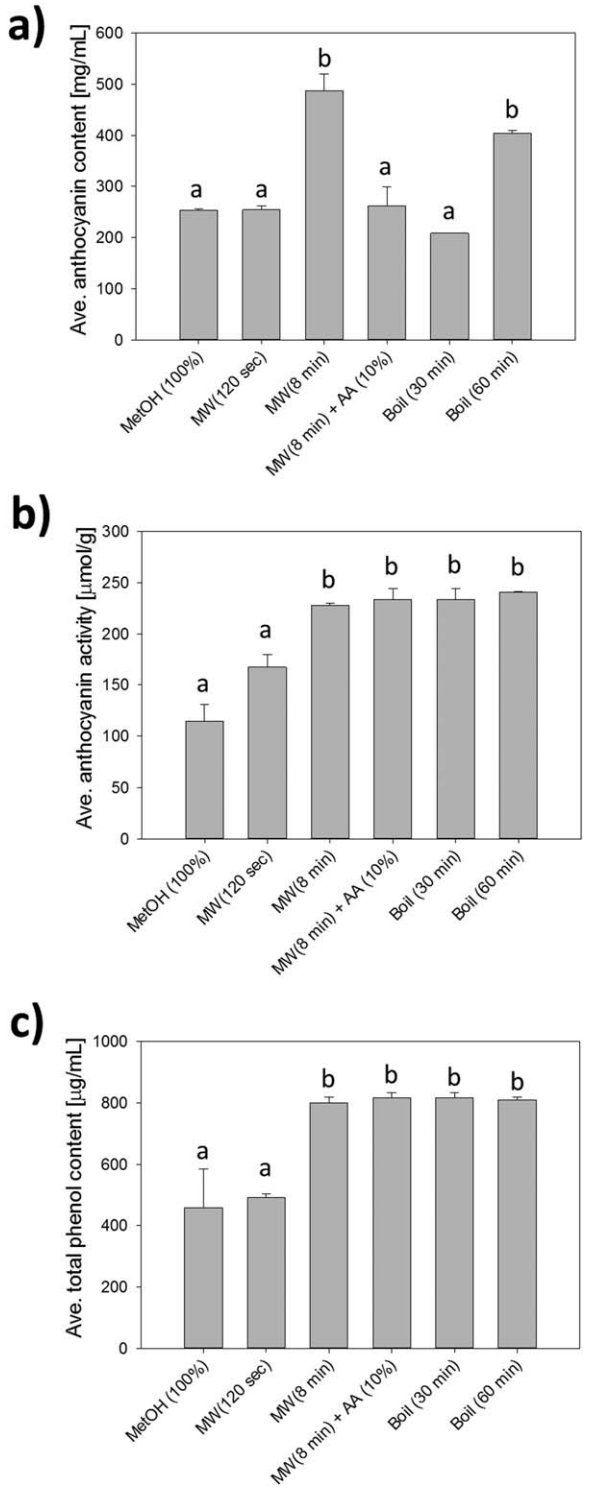

Figure 1. Comparison of the best extraction methods used in this study for anthocyanin content (a), antioxidant activity (b), and total phenol content (c). Other methods can be found in the supplemental section. Different lower case letters denote statistically different groups (ANOVA, $\alpha = 0.05$).

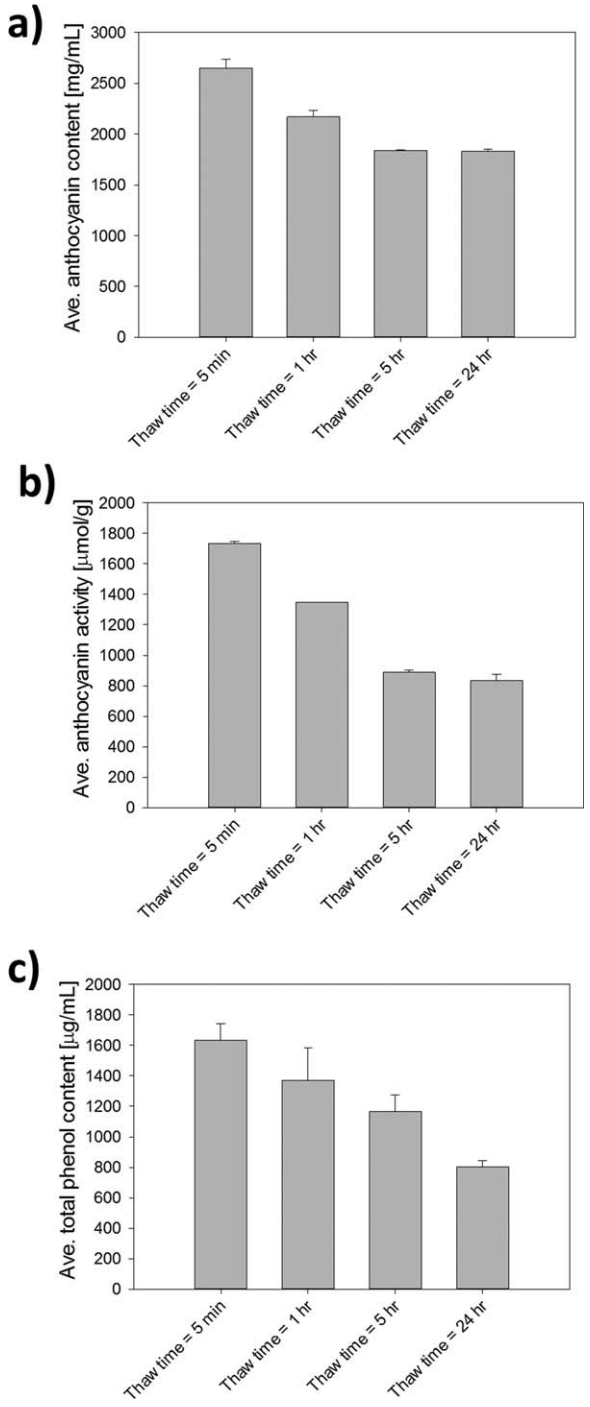

Figure 2. Photochemical behavior for various extraction methods.

(a) UV VIS spectra (λ_{Ex} = 280 nm) for cryoconcentrated extract at various pH. (b) Average peak intensity at 420, 450, and 640 nm for cryoconcentrated extract (λ_{Ex} = 280 nm). (c) Representative UV VIS spectra for boiled extract, microwave with acetic acid (MW + AA), and cryoconcentrated extract (λ_{Ex} = 300 nm); photograph shows color of extract after extraction. (d) Average peak intensity for various extraction methods shown in c for an excitation of 300 nm. The absorption intensity for cryoconcentrated extract was significantly higher than all other methods ($P \leq 0.01$, $\alpha = 0.05$).

extract that was boiled for 60 min (1420 a.u.; CIE = 550). Although temperatures of 100°C can indeed denature extract proteins[57] and anthocyanin,[58] boiling produced the optimal result when considering anthocyanin content, antioxidant activity, total phenol concentration, absorption, and total cost. Preliminary analysis with dye-sensitized solar cells (DSSC) and pH-sensitive thin films showed that extraction at non-neutral pH (methanol extraction) or using microwave irradiation (with or without AA) resulted in lower phenol and anthocyanin relative to boiling for 60 min (for photos of extracts see inset in Figure 2c). Although the specific molecular mechanism for this reduction in DSSC/sensor efficiency

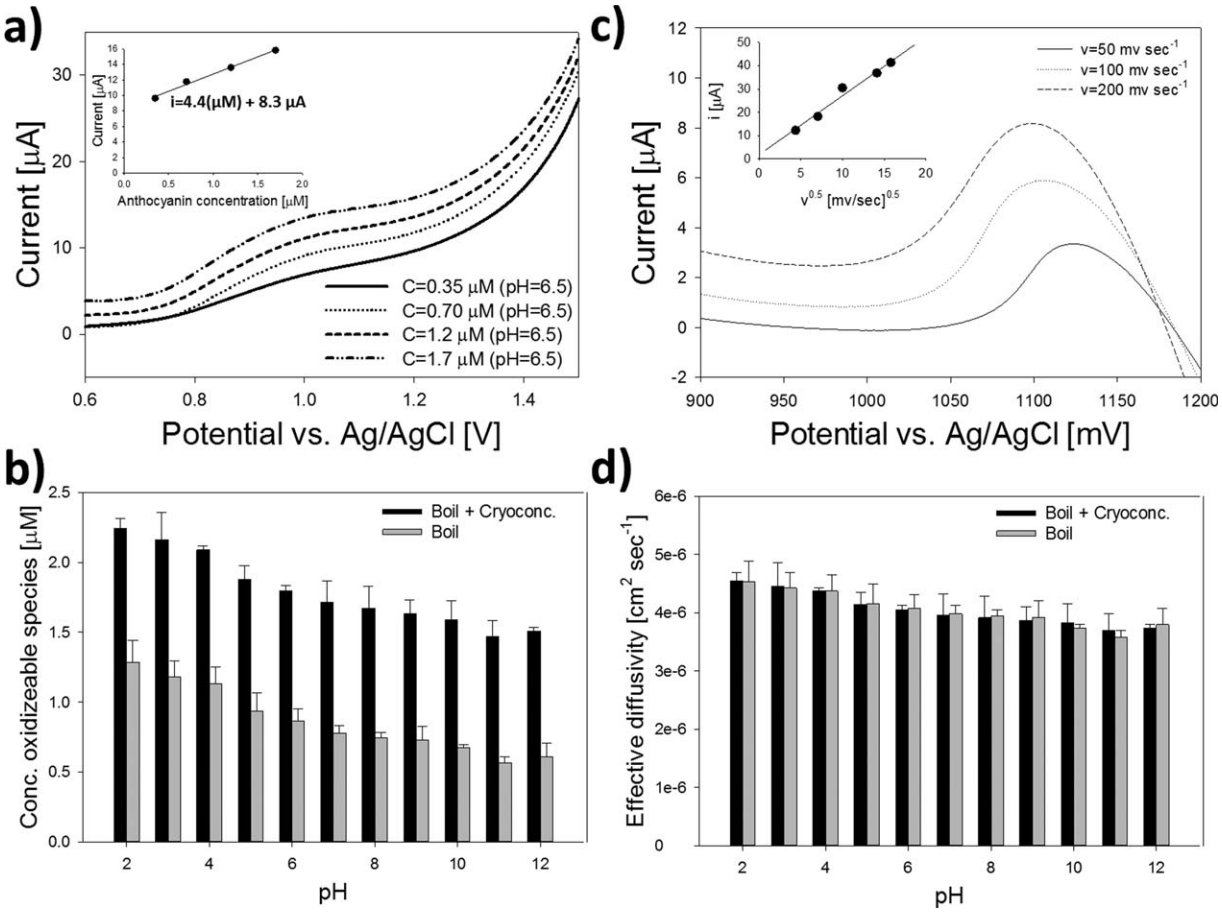

Figure 3. Effect of thawing time on cryoconcentrated extract, including: anthocyanin content (a), antioxidant activity (b), and total phenol content (c). The highest concentration of each was recorded after 5 min of thawing, which decreased at an average rate of 0.6 ± 0.2 h^{-1}. Different lower case letters denote statistically different groups (ANOVA, $\alpha = 0.05$).

is not known, this result is most likely due to the presence of compounds not analyzed by the assays used in this study as the CIE data indicate clear differences in the pigmentation of each extract. Other established techniques such as adsorption column separation could be used to improve the purification of the extract, removing impurities such as sugars, organic acids, and proteins,[14] but these techniques can be cost prohibitive in many applied settings, such as development of low cost sensors.

To improve the extraction yield, block cryoconcentration followed by passive partial thawing was used (Figure 3). Miyawaki[59] showed that passive (i.e., gravitational) partial thawing of the cryoconcentrated block is optimal for high solute concentrations, while final freezing temperature had no effect on extract yield. Anthocyanin content/antioxidant activity and total phenol content were measured over time during passive thawing. After 5 min at 20°C, the anthocyanin content (2649 ± 83 mg/mL), antioxidant activity (1635 ± 106 μmol g^{-1}) and total phenol content (1732 ± 14 μg/g) of the extract were significantly higher than all other methods tested ($P < 0.01$, $\alpha = 0.05$). As expected, these values decreased exponentially as the frozen extract was diluted by melting ice. Anthocyanin content and antioxidant activity (0.6 ± 0.2 and 0.2 ± 0.1 h, respectively) decreased at a lower rate than the total phenol (1.0 ± 0.3 h). Surprisingly, after 24 h at 20°C, the extract was fully thawed and the anthocyanin content/activity was higher than extract prepared by boiling in water for 1 h ($P = 0.010$, $\alpha = 0.05$), although the total phenol content was not statistically different ($P = 0.13$, $\alpha = 0.05$). We speculate that the marked difference in dilution by water is the main reason for the increased phenol content and anthocyanin activity in the extract, although the specific mechanism is not known at this time. Aider and de Halleux[33] showed that, other than the total time to thaw, there was no difference between microwave-assisted thawing or passive thawing of cryoconcentrated maple sap extract (the study measured sugar content, electroconductivity, and CIE chromaticity). However, in our work we saw a clear difference in the extracts taken at different times during passive block thawing.

The results in Figures 1–3 indicate that boiling for one hour followed by cryoconcentration enhances extraction efficiency considerably. Our study did not use vacuum-assisted cryoconcentration or tubular ice systems for progressive cryoconcentration due to the added expense and need for additional equipment, although both methods may possibly improve extraction efficiency. Petzold et al.[37] showed that the time for cryoconcentration can be reduced by up to 33% if a vacuum system is used. Gunathilake et al.[60] and Miyawaki et al.[61] showed that tubular ice systems for partial ice melting enhance extraction efficiency by up to 20% relative to progressive cryoconcentration and passive thawing. The technique here is a simple, highly efficient green method for obtaining highly concentrated anthocyanin at physiological pH and salinity.

Extract electrochemistry

Figure 4a shows a representative linear sweep voltammogram (LSV) at various extract concentrations (pH = 7). The

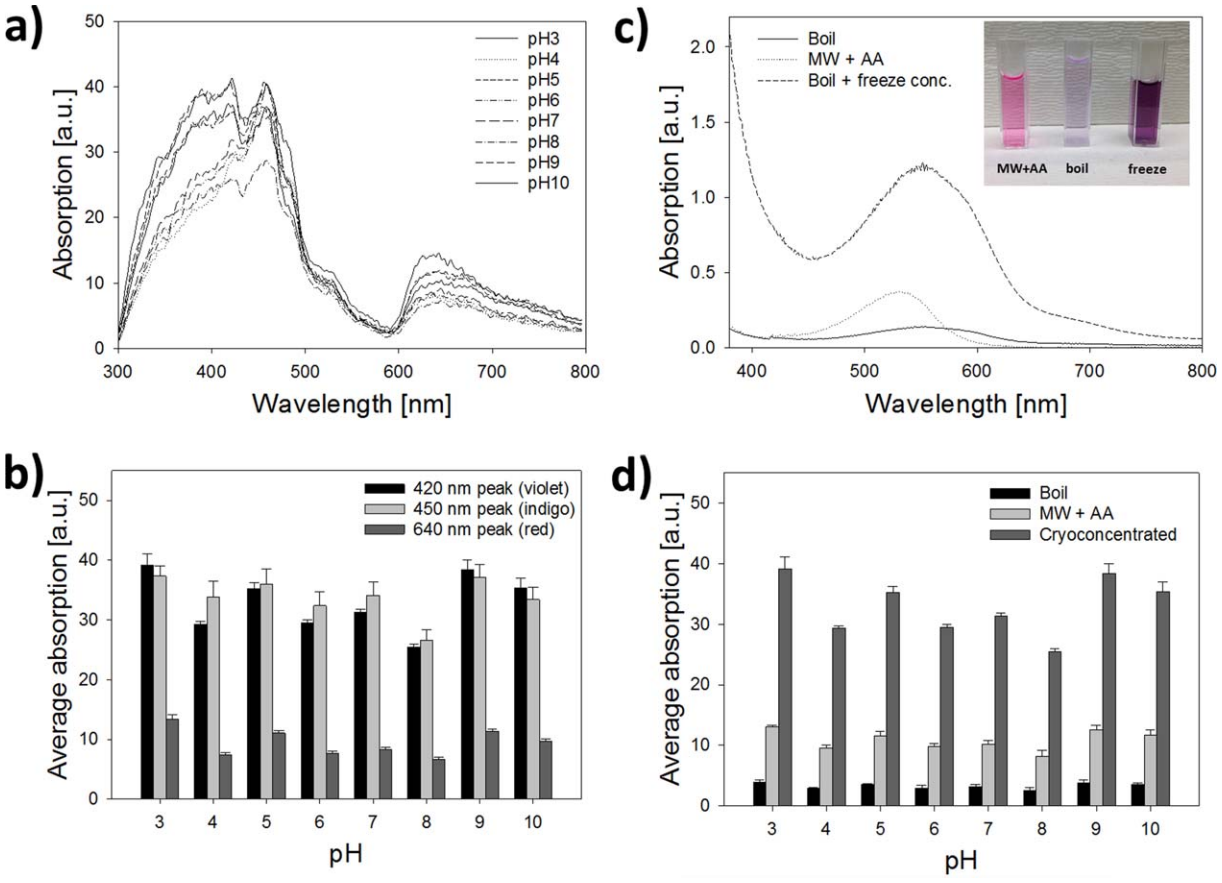

Figure 4. Electrochemical behavior of extract with and without cryoconcentration (sample taken 5 min after placing frozen extract at 20°C).

(a) A representative linear sweep voltammogram (LSV) at various concentrations of cryoconcentrated extract (pH = 7). Inset shows peak current at various anthocyanin concentrations. (b) Average concentration of oxidizeable species calculated from LSV data. (c) Representative cyclic voltammogram (CV) at various scan rates (pH 7). Inset shows Cottrell plot indicating a linear increase in peak oxidation current with the square root of the scan rate. (d) Effect of pH on diffusion coefficient with and without cryoconcentration.

inset shows the relationship between average oxidative peak current and total concentration of oxidizable species, which increases linearly as expected. As the pH increased, the oxidation potential decreased (Figure 4b), indicating that flavonoids are easily oxidized at higher pH as hydroxyl groups are deprotonated in accordance with the Nernst law (slope = 58 ± 3 V/pH). At all pH levels tested, the cryoconcentrated extract had a significantly higher concentration of oxidizeable species than boiled extract ($P < 0.0001$, $\alpha = 0.05$), which is similar to the trend in Figure 1. In addition, the extract was more stable at lower pH, based on the results shown here. The oxidation potential at 1 V is associated with electrochemical oxidation of flavonoids (FL-OH → FL-O• + e^- + H^+); where FL is a flavonoid.[45] The electrochemical data in Figure 4a,b and antioxidant activity measured by radical scavenging (DPPH) from Figure 1b (FL-OH → FL-O• + H^+) are tightly correlated since each technique reports data based on the same hydroxyl groups on the anthocyanin.

Figure 4c shows the oxidative sweep of a representative cyclic voltammogram (CV) at various scan rates for an extract concentration of 1.7 μM and pH = 7. The oxidation peak near 1 V confirms that functional hydroxyl groups on anthocyanin were electrochemically oxidized at the electrode surface. Based on the work by Lima et al.,[45] the relatively high oxidation potential corresponds to C-3 hydroxyl groups, resornicol groups, and the presence of sugars in the ring structure. The inset in Figure 4c shows a linear Cottrell plot, indicating that transport was diffusion limited, as expected. Using the Randles–Sevcik theorem, the diffusion coefficient (D) was calculated at various pH levels; data shown for cryoconcentrated extract and boiled extract are shown in Figure 4d. For both extracts, the value of D slightly decreased as the pH increased, which was also shown by Xavier et al.[62] The net change in diffusion coefficient from pH 3 to pH 7 (12.9 ± 2.1%) was more significant than the net change from pH 7 to pH 11 (5.7 ± 1.6%). This is most likely attributed to nonacylated anthocyanins (comprising 20–30% of total anthocyanins) and methylated anthocyanins (e.g., peonidin), which are sensitive to pH changes. There was no significant difference between the two extraction procedures with regards to diffusion coefficient at all pH levels tested ($P < 0.0001$, $\alpha = 0.05$). This electrochemical characterization confirms that the cryoconcentrated extract has potential application as a dye in electrochemical devices.

Extract photochemistry

Aqueous extracts of anthocyanin are known to undergo a variety of resonant structural transformations when the pH of the solution changes, which is the major driving force for observed color changes.[63] At low pH (3–4), the anthocyanin was protonated (i.e., flavylium salt) and appeared red in color with a CIE chroma of 496. See Supporting Information

Figure S5 for photographs and CIE chroma of extract at various pH levels. The peak absorption for pH 3–4 was at 420 nm for an excitation of 250 nm, followed by a broad peak between 600 and 700 nm (Figure 2a,b). As pH was increased to the 4–5 range, a slow color transition occurred as the anthocyanin adopted a carbinol structure; some anthocyanins are known to be colorless in this state while others are pink with a CIE chroma of 528.[63] The peaks at 420, 450, and 640 nm all decreased during this slow carbinol transition. Slight bathochromic shifts occurred as pH increased, although this change was not significant. At neutral pH, the anthocyanin was rapidly deprotonated and in the anhydro base conformation (appearing bluish purple in color with a CIE chroma of 555). The peaks at 420 and 540 nm decreased considerably, while the peak at 450nm did not change significantly compared with the flavylium and carbinol structures. When the pH was increased to 10, a slow transition to the chalcone conformation was obtained as the ring structure opened, and the solution appeared green with a CIE chroma of 485. Above pH 10 the color of the solution was dark yellow with a chroma of 572, the peaks at 420 and 640 nm increased (similar to carbinol peaks), while the peak at 450 nm did not change. As described by Gomes et al.,[21] kinetics of these structural transitions play a major role in the photochemical behavior. For the fast deprotonation conformational transitions at pH 3,6,7, and 8 there was a linear relationship between pH and UV absorption for the 420 nm peak ($R^2 = 0.90$), 450 nm peak ($R^2 = 0.82$), and 640 nm peak ($R^2 = 0.92$). However, for the slow transition to carbinol and chalcone resonant structures, there was no linear relationship between peak intensity and pH. Figure 2d shows that the average peak absorbance for the cryoconcentrated extract was significantly higher than other methods ($P < 0.0001$, $\alpha = 0.05$), indicating that the extract has excellent potential for colorimetric biosensing.

Proof of principle applications

As discussed in detail by Hug et al.,[52] DSSC have been developed with a variety of anthocyanins, including extract from *B. oleracea*, black rice (*Oryza sativa*), Manchu rose (*Rosa xanthina*), spiderwort (*Tradescantia zebrine*), and *Rhododendron*, among others. Figure 5a shows the electrochemical behavior (*I–E* curve) and power output of a DSSC at various illumination levels with and without cryoconcentration. The short circuit current density (J_{SC}), open circuit potential (E_{OC}), maximum power output (P_{max}), and solar conversion efficiency (η) increased with increasing illumination, as expected (see Supporting Information Tables S1–S2 for details). The form factor (FF) for all DSSC was not significantly different, but all other solar power conversion parameters were significantly higher for cryoconcentrated extract compared with boiled extract ($P = 0.001$, $\alpha = 0.05$). These results are similar to other DSSC reviewed by Hug et al.,[52] most of which used pretreatment methods, expensive materials, or complex electrodes. On the other hand, our device was developed by simply concentrating the anthocyanin and using simple assembly methods as described in detail by Furukawa et al.[64] The highest efficiency was measured for DSSC prepared with cryoconcentrated extract at an illumination of 200 mW (49%), which was over four times higher than the efficiency of DSSC prepared with boiled extract. This shows a clear relationship between anthocyanin content, antioxidant activity (recall Figure 1) and DSSC

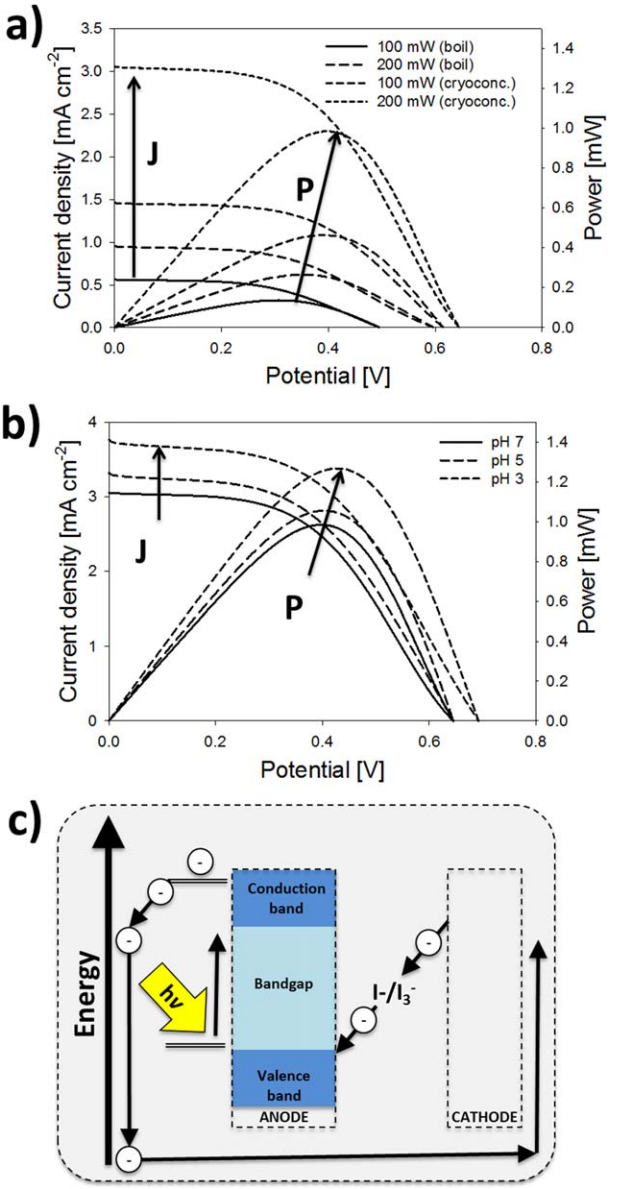

Figure 5. Demonstration of DSSC based on cryoconcentration when compared with heat extraction (boiling).

(a) Current–potential (*I–E*) curve and power curve for a flavonoid-sensitized solar cell. (b) *I–E* and power curve for cryoconcentrated extract at various pH levels, showing an increase in power output with decreasing pH. (c) Schematic of energy diagram for DSSC depicting electron transfer between the anode and cathode using iodide as the electrolyte.

performance, which is similar to the work by Hemmatzadeh et al.[65] comparing various solvent extraction techniques for DSSC (including ethanol extraction and heat extraction). In addition to the effect of anthocyanin content on DSSC performance, pH also plays an important role in DSSC. Figure 5b shows that efficiency increased by 20% when the pH was decreased from 7 to 3 due to electron injection at the metal oxide surface using boronic acid as a dye anchor to the metal oxides.[66]

Although we did not test the effect of immersion time on performance (anodes were immersed for 30 min in this study), Li et al.[67] showed that DSSC power increases with time as the anode is immersed in extract for longer periods, with maximum power measured after 24 h, implying a

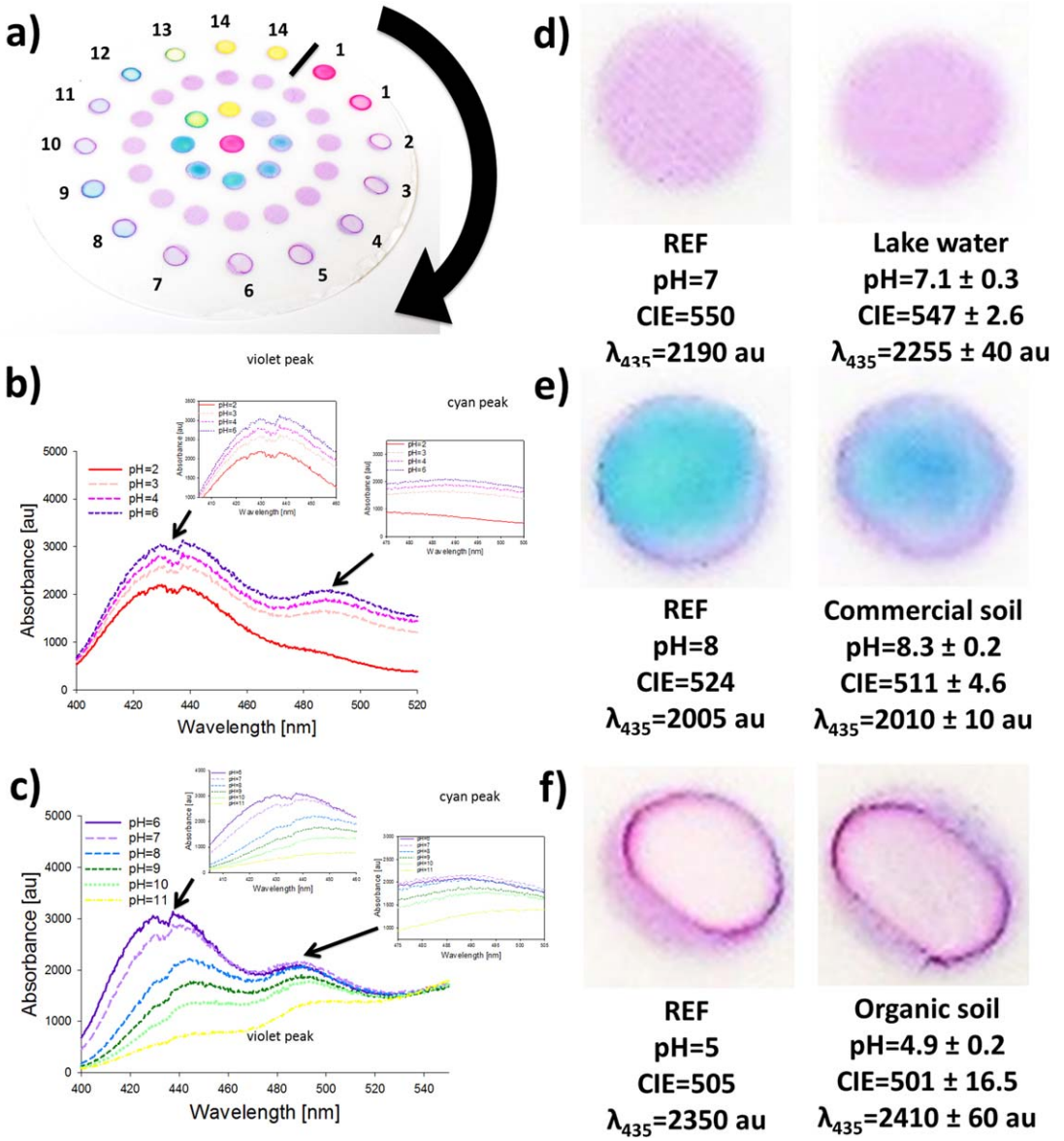

Figure 6. Inkjet-printed red cabbage extract on nanocellulose substrate in a circular array for pH sensing.

(a) Photograph of inkjet-printed "dots" on a circular disc. The outer ring represents pH increasing clockwise from 1 to 14, the middle ring represents control samples (pH 7), the third ring represents increase of pH clockwise from 7 to 14, and the middle circle is pH 1. (b) UV–VIS spectra for pH 2 to pH 6; (c) VIS spectra for pH 6–11. The pH-sensitive film was applied for analyzing water samples from (d) a fresh water lake, (e) a commercial soil, and (f) an organic soil. CIE and peak absorption at 435 nm are shown for each thin film. Reference image (buffers) are shown for comparison.

concentration dependence. Since the DSSC efficiency depends on the concentration of flavonoids, the cryoconcentration method is a highly useful and simple mechanism for enhancing DSSC performance. In the future, DSSC can be further improved by deposition of nanocrystalline TiO_2 films,[68] use of plastic substrates such as polyethylene napthalate,[69] or by mixing extracts from multiple plant species such as red cabbage and blueberry.[70] Figure 5c shows the energy pathway for the electrochemical cell, and a detailed schematic of the working mechanism can be seen in Supporting Information Figure S1. These results clearly show that cryoconcentration of extract enhances DSSC performance when compared with boiled extract.

Figure 6 shows the performance of inkjet-printed biodetectors for direct measurement of pH. Figure 6a shows a photograph of the inkjet-printed "dots" at pH from 1 to 14 (outer ring). The middle ring of dots shows a control (pH = 7), the inner ring shows standards of pH 14–7, and the innermost dot is pH 1. The color of the films in Figure 6 are nearly identical to the trend in Figure 2; red at pH < 4, blue at pH 5–6, purple at pH 7, blue/green at pH 8–9, and green/yellow above pH 10. In Figure 6b,c, the UV–VIS spectra are shown (white light excitation) for pH 2–6. The violet peak (435 nm) and cyan peak (480 nm) also followed the same trends in Figure 2, although the bathochromic shifts were more pronounced than when the anthocyanin was suspended in aqueous solution. Figure 6d–f shows applications of the printed anthocyanin using samples from lake water (Figure 5d), commercial soil (Figure 6e), and organic soil (Figure 6f). In each case, the reference image from Figure 6a, the measured CIE, and the absorbance (λ_{Ex} = 435 nm) are shown for comparison. For each of the samples, the pH

measured with a standard electrode was within ± 0.5 pH units (see Supporting Information Table S3 for details). These results demonstrate that the inkjet-printed films are applicable for rapid field monitoring of solution pH in samples relevant to agricultural, ecological, and environmental studies.

In addition to the proof of principle demonstrations herein, our previous work has shown that anthocyanin can be used to synthesize nanoparticles[12] or for functional foods,[9] and Castañeda-Ovando et al.[4] discuss a variety of other applications such as cosmetic and pharmaceutical uses. We have shown the simple extraction and cryoconcentration of anthocyanin from *B. oleracea* using block cryoconcentration with partial gravitational thawing as an effective method for creating value added products. In addition to producing highly stable extract with attractive properties, the leaves are intact after boiling, and could be consumed or used as a food product, when compared with solvent extraction methods which destroy the food product. Other applications not discussed in detail here include use of cabbage extract as a biosorbent[71] and cancer preventative medicines.[72] The low cost, simple method can be created in any lab without the use of specialty equipment.

Conclusion

There is a need for sustainable value added products and technologies derived from agricultural materials. Among the diverse library of bioderived materials from agricultural feedstocks, flavonoids, including anthocyanins, are among one of the most promising due to low cost and land use at the farm scale. In this work, we show that cryoconcentration of leaf extract from red cabbage (*B. oleracea*) is a facile, low cost, green approach for producing large quantities of anthocyanin. The extract has excellent photochemical and electrochemical stability, and can be used in a number of applications. To demonstrate this concept, two proof of principle technologies were fabricated and tested (a dye sensitized solar cell and a thin film biodetector). These results clearly show that cryoconcentration of *B. oleracea* leaf extract is a useful method that can be used to develop biotechnologies such as solar cells and sensors. Future research will investigate the stability of cabbage extract from cryoconcentration compared to other methods for creating value added products.

Acknowledgments

The authors acknowledge the UF Student Science Training Program (KG), the Colombian funding agencies Colfuturo y Colciencias (DV-No.001375882), the Agricultural and Biological Engineering Department at the University of Florida (ESM-USDA/NIFA Hatch Project No. FLA-ABE-005062), the Turkish Ministry of National Education (AD),the National Institute of Food and Agriculture, US Department of Agriculture, under award number 11901762 (JCC); the Iowa State University College of Engineering and Department of Mechanical Engineering(JCC), and the USDA Multistate Project (NC1194) for financial support. The authors also thank Y. Yagiz from the Food and Environmental Toxicology Lab (FETL) in the Department of Food Science and Human Nutrition at the University of Florida for assistance with antioxidant testing.

Literature Cited

1. Briggs WR, Liscum E. The role of mutants in the search for the photoreceptor for phototropism in higher plants. *Plant Cell Environ.* 1997;20:768–772.
2. Masclaux-Daubresse C, Chardon F. Exploring nitrogen remobilization for seed filling using natural variation in *Arabidopsis thaliana*. *J Exp Bot.* 2011;62:2131–2142.
3. González-Teuber M, Heil M. Nectar chemistry is tailored for both attraction of mutualists and protection from exploiters. *Plant Signal Behav* 2009;4:809–813.
4. Castaneda-Ovandode Pacheco-Hernnndez Lourdes AM, Paez-Hernandez ME, Rodriguez JA, Galnn-Vidal Andres C. Chemical studies of anthocyanins: a review. *Food Chem.* 2009;113:859–871.
5. Dang K-V, Plet J, Tolleter D, Jokel M, Cuiné S, Carrier P, Auroy P, Richaud P, Johnson X, Alric J, Allahverdiyeva Y, Peltier G. Combined increases in mitochondrial cooperation and oxygen photoreduction compensate for deficiency in cyclic electron flow in *Chlamydomonas reinhardtii*. *Plant Cell* 2014;26:1–16.
6. Fossen T, Cabrita L, Andersen OM. Colour and stability of pure anthocyanins influenced by pH including the alkaline region. *Food Chem.* 1998;63:435–440.
7. Dyrby M, Westergaard N, Stapelfeldt H. Light and heat sensitivity of red cabbage extract in soft drink model systems. *Food Chem.* 2001;72:431–437.
8. Walkowiak-Tomczak D, Czapski J. Colour changes of a preparation from red cabbage during storage in a model system. *Food Chem.* 2007;104:709–714.
9. Wang J, Huang Y, Li K, Chen Y, Vanegas DC, McLamore ES, Shen Y. Leaf extracts from *Lithocarpus polystachyus* Rehd. promote glycogen synthesis in T2DM mice. *PLoS One*. DOI:10.1371/journal.pone.0166557, 2016.
10. Nabavi SF, Habtemariam S, Daglia M, Shafighi N, Barber AJ, Nabavi SM. Anthocyanins as a potential therapy for diabetic retinopathy. *Curr Med Chem.* 2015;22:51–58.
11. Xie Y, Kocaefe D, Chen C, Kocaefe Y. Review of research on template methods in preparation of nanomaterials. *J Nanomater*. 2016;2016:1–10.
12. Demirbas A, Welt BA, Ocsoy I. Biosynthesis of red cabbage extract directed Ag NPs and their effect on the loss of antioxidant activity. *Mater Lett*. 2016;179:20–23.
13. AnangaGeorgiev A, Ochieng V, Phills JB, Tsolov V. Production of anthocyanins in grape cell cultures: a potential source of raw material for pharmaceutical, food, and cosmetic industries. *Mediterr Genet Code Grapevine Olive*. 2013;247–287.
14. Jampani C, Raghavarao KSMS. Process integration for purification and concentration of red cabbage (*Brassica oleracea* L.) anthocyanins. *Sep Purif Technol*. 2015;141:10–16.
15. Zhu H, Zeng H, Subramanian V, Masarapu C, Hung K-H, Wei B. Anthocyanin-sensitized solar cells using carbon nanotube films as counter electrodes. *Nanotechnology* 2008;19:465204.
16. Siedler S, Stahlhut SG, Malla S, Maury J, Neves AR. Novel biosensors based on flavonoid-responsive transcriptional regulators introduced into *Escherichia coli*. *Metab Eng*. 2014;21:2–8.
17. Dhale R, Dhongade V, Aiyer RC, Kodam K. Anthocyanin coated carbon dioxide biosensor. *2nd Int Symp Phys Technol Sens*. 2015;8–10.
18. Diaz JT, Chinn MS, Den Truong V. Simultaneous saccharification and fermentation of industrial sweetpotatoes for ethanol production and anthocyanins extraction. *Indus Crops Prod*. 2014;62:53–60.
19. Kautsky H, Hirsch A. Energie-Umwandlungen an Grenzflächen, IV. *Ber Dtsch Chem Ges B* 64:2677–2683.
20. Chen H, Yada R. Nanotechnologies in agriculture: new tools for sustainable development. *Trends Food Sci Technol*. 2011;22:585–594.
21. Gomes R, Parola AJ, Lima JC, Pina F. Solvent effects on the thermal and photochemical reactions of 4-Iodo-8-methoxyflavylium and their consequences on the coloring phenomena caused by anthocyanins in plants. *Chem A Eur J*. 2006;12:7906–7912.
22. Quina FH, Moreira PF, Vautier-Giongo C, Rettori D, Rodrigues RF, Freitas AA, Silva PF, Maçanita AL. Photochemistry of

anthocyanins and their biological role in plant tissues. *Pure Appl Chem* 2009;81:1687–1694.
23. Drabent R, Pliszka B, Olszewska T. Fluorescence properties of plant anthocyanin pigments. I. Fluorescence of anthocyanins in *Brassica oleracea* L. extracts. *J Photochem Photobiol B Biol*. 1999;50:53–58.
24. Roshchina VV, Roshchina VV. Vital autofluorescence: application to the study of plant living cells. *Int J Spectrosc*. 2012; 2012:1–14.
25. Bennett MD, Price HJ, Johnston JS. Anthocyanin inhibits propidium iodide DNA fluorescence in *Euphorbia pulcherrima*: implications for genome size variation and flow cytometry. *Ann Bot*. 2008;101:777–790.
26. Charron CS, Clevidence BA, Britz SJ, Novotny JA. Effect of dose size on bioavailability of acylated and nonacylated anthocyanins from red cabbage (*Brassica oleracea* L. Var. capitata). *J Agric Food Chem*. 2007;55:5354–5362.
27. Arapitsas P, Turner C. Pressurized solvent extraction and monolithic column-HPLC/DAD analysis of anthocyanins in red cabbage. *Talanta* 2008;74:1218–1223.
28. Lu LZ, Zhou YZ, Zhang YQ, Ma YL, Zhou LX, Li L, Zhou ZZ, He TZ. Anthocyanin extracts from purple sweet potato by means of microwave baking and acidified electrolysed water and their antioxidation *in vitro*. *Int J Food Sci Technol*. 2010; 45:1378–1385.
29. Khoddami A, Wilkes MA, Roberts TH. Techniques for analysis of plant phenolic compounds. *Molecules* 2013;18:2328–2375.
30. Demirdöven A, Özdoğan K, Erdoğan-Tokatlı K. Extraction of anthocyanins from red cabbage by ultrasonic and conventional methods: optimization and evaluation. *J Food Biochem*. 2015; 39:491–500.
31. Gachovska T, Cassada D, Subbiah J, Hanna M, Thippareddi H, Snow D. Enhanced anthocyanin extraction from red cabbage using pulsed electric field processing. *J Food Sci*. 2010;75:323–329.
32. Park S, Arasu MV, Jiang N, Choi SH, Lim YP, Park JT, Al-Dhabi NA, Kim SJ. Metabolite profiling of phenolics, anthocyanins and flavonols in cabbage (*Brassica oleracea* var. capitata). *Indus Crops Prod*. 2014;60:8–14.
33. Aider M, de Halleux D. Passive and microwave-assisted thawing in maple sap cryoconcentration technology. *J Food Eng*. 2008;85:65–72.
34. Aider M, de Halleux D, Melnikova I. Gravitational and microwave-assisted thawing during milk whey cryoconcentration. *J Food Eng*. 2008;88:373–380.
35. Aider M, de Halleux D. Production of concentrated cherry and apricot juices by cryoconcentration technology. *LWT Food Sci Technol*. 2008;41:1768–1775.
36. Petzold G, Orellana P, Moreno J, Cerda E, Parra P. Vacuum-assisted block freeze concentration applied to wine. *Innov Food Sci Emerg Technol*. 2016;36:330–335.
37. Petzold G, Aguilera JM. Centrifugal freeze concentration. *Innov Food Sci Emerg Technol*. 2013;20:253–258.
38. Gulfo R, Auleda JM, Moreno FL, Ruiz Y, Hernández E, Raventós M. Multi-plate freeze concentration: recovery of solutes occluded in the ice and determination of thawing time. *Food Sci Technol Int*. 2014;20:405–419.
39. Cissé Vaillant MF, Pallet D, Dornier M. Selecting ultrafiltration and nanofiltration membranes to concentrate anthocyanins from Roselle extract (*Hibiscus sabdariffa* L.). *Food Res Int*. 2011;44: 2607–2614.
40. Lee J, Durst RW, Wrolstad RE. Determination of total monomeric anthocyanin pigment content of fruit juices, beverages, natural colorants, and wines by the pH differential method: collaborative study. *J AOAC Int*. 2005;88:1269–1278.
41. Brand-Williams W, Cuvelier ME, Berset C. Use of a free radical method to evaluate antioxidant activity. *LWT Food Sci Technol*. 1995;28:25–30.
42. Milan SS. Total phenolic content, flavonoid concentration and antioxidant activity of *Marrubium peregrinum* L. extracts. *Kragujev J Sci*. 2011;33:63–72.
43. Piljac-Žegarac J, Stipčević2 T, Belščak A. Antioxidant properties and phenolic content of different floral origin honeys. *J ApiProduct ApiMed Sci*. 2009;1:43–50.
44. Aguirre MJ, Chen YY, Isaacs M, Matsuhiro B, Mendoza L, Torres S. Electrochemical behaviour and antioxidant capacity of anthocyanins from Chilean red wine, grape and raspberry. *Food Chem*. 2010;121:44–48.
45. de Lima A, Sussuchi EM, Giovani WFD. Electrochemical and antioxidant properties of anthocyanins and anthocyanidins. *Croat Chem Acta* 2007;80:29–34.
46. Moncada MC, de Mesquita MF, dos Santos MMC. Electrochemical oxidation of the synthetic anthocyanin analogue 4-methyl-7,8-dihydroxyflavylium salt. *J Electroanal Chem*. 2009;636:60–67.
47. Vanegas DC, Taguchi M, Chaturvedi P, Burrs S, Tan M, Yamaguchi H, McLamore ES. A comparative study of carbon–platinum hybrid nanostructure architecture for amperometric biosensing. *Analyst* 2014;139:660–667.
48. Chaturvedi P, Vanegas DC, Taguchi M, Burrs SL, Sharma P, McLamore ES. A nanoceria-platinum-graphene nanocomposite for electrochemical biosensing. *Biosens Bioelectron*. 2014;58: 179–185.
49. Burrs SL, Vanegas DC, Bhargava M, Mechulan N, Hendershot P, Yamaguchi H, Gomes C, McLamore ES. A comparative study of graphene-hydrogel hybrid bionanocomposites for biosensing. *Analyst* 2015;140:1466–1476.
50. McLamore ES, Shi J, Jaroch D, Claussen JC, Uchida a, Jiang Y, Zhang W, Donkin SS, Banks MK, Buhman KK, Teegarden D, Rickus JL, Porterfield DM. A self referencing platinum nanoparticle decorated enzyme-based microbiosensor for real time measurement of physiological glucose transport. *Biosens Bioelectron*. 2011;26:2237–2245.
51. Kumar S, McEvoy N, Lutz T, Keeley GP, Nicolosi V, Murray CP, Blau WJ, Duesberg GS. Gas phase controlled deposition of high quality large-area graphene films. *Chem Commun. (Camb)* 2010;46:1422–1424.
52. Hug H, Bader M, Mair P, Glatzel T. Biophotovoltaics: natural pigments in dye-sensitized solar cells. *Appl Energy* 2014;115: 216–225.
53. He Q, Das SR, Garland NT, Jing D, Hondred JA, Cargill AA, Ding S, Karunakaran C, Claussen JC. Enabling inkjet printed graphene for ion selective electrodes with post-print thermal annealing. *ACS Appl Mater Interfaces*. DOI:10.1021/acsami.7b0009, 2017.
54. Das SR, Uz M, Ding S, Lentner MT, Hondred JA, Cargill AA, Sakaguchi DS, Mallapragada S, Claussen JC. Electrical differentiation of mesenchymal stem cells into Schwann-cell-like phenotypes using inkjet-printed graphene circuits. *Adv Heal Mater*. DOI: 10.1002/adhm.201601087.
55. Das SR, Nian Q, Cargill AA, Hondred JA, Ding S, Saei M, Cheng GJ, Claussen JC. 3D nanostructured inkjet printed graphene via UV-pulsed laser irradiation enables paper-based electronics and electrochemical devices. *Nanoscale* 2016;8:15870–15879.
56. Miller RO, Kissel DE. Comparison of soil pH methods on soils of North America. *Soil Sci Soc Am J*. 2010;74:310.
57. Aider M, de Halleux D, Akbache A. Whey cryoconcentration and impact on its composition. *J Food Eng*. 2007;82:92–102.
58. Arkoub-DjermouneBoulekbache-Makhlouf L, Zeghichi-Hamri L, Bellili S, Boukhalfa SF, Madani K. Influence of the thermal processing on the physico-chemical properties and the antioxidant activity of a solanaceae vegetable: eggplant. *J Food Qual* 2016.
59. Miyawaki O, Kato S, Watabe K. Yield improvement in progressive freeze-concentration by partial melting of ice. *J Food Eng*. 2012;108:377–382.
60. Gunathilake M, Dozen M, Shimmura K, Miyawaki O. An apparatus for partial ice-melting to improve yield in progressive freeze-concentration. *J Food Eng*. 2014;142:64–69.
61. Miyawaki O, Gunathilake M, Omote C, Koyanagi T, Sasaki T, Take H, Matsuda A, Ishisaki K, Miwa S, Kitano S. Progressive freeze-concentration of apple juice and its application to produce a new type apple wine. *J Food Eng*. 2016;171:153–158.
62. Xavier MF, Lopes TJ, Quadri MGN, Quadri MB. Extraction of red cabbage anthocyanins: optimization of the operation conditions of the column process. *Braz Arch Biol Technol*. 2008;51: 143–152.

63. Olivas-Aguirre FJ, Rodrigo-Garcia J, Martinez-Ruiz NDR, Cardenas-Robles AI, Mendoza-Diaz SO, Alvarez-Parrilla E, Gonzlez-Aguilar GA, De La Rosa LA, Ramos-Jiméinez A, Wall-Medrano A. Cyanidin-3-*O*-glucoside: physical-chemistry, foodomics and health effects. *Molecules* 2016;21.
64. Furukawa S, Iino H, Iwamoto T, Kukita K, Yamauchi S. Characteristics of dye-sensitized solar cells using natural dye. *Thin Solid Films* 2009;518:526–529. no. p
65. Hemmatzadeh R, Jamali A. Enhancing the optical absorption of anthocyanins for dye-sensitized solar cells: enhancing the optical absorption of anthocyanins for dye-sensitized solar cells. *J Renew Sustain Energy* 2015;13120.
66. Zhang L, Cole JM. Anchoring groups for dye-sensitized solar cells. *ACS Appl Mater Interfaces* 2015;7:3427–3455.
67. Li M, Liu Y, Wang H, Shen H. Synthesis of TiO_2 submicrorings and their application in dye-sensitized solar cell. *Appl Energy* 2011;88:825–830.
68. Gokilamani N, Muthukumarasamy N, Thambidurai M, Ranjitha A, Velauthapillai D. Utilization of natural anthocyanin pigments as photosensitizers for dye-sensitized solar cells. *J Sol-Gel Sci Technol*. 2013;66:212–219.
69. Yoo K, Kim JY, Lee JA, Kim JS, Lee DK, Kim K, Kim JY, Kim B, Kim H, Kim WM, Kim JH, Ko MJ. Completely transparent conducting oxide-free and flexible dye-sensitized solar cells fabricated on plastic substrates. *ACS Nano*.2015;9:3760–3771.
70. Syafinar R, Gomesh N, Irwanto M, Fareq M, Irwan YM. Potential of purple cabbage, coffee, blueberry and turmeric as nature based dyes for dye sensitized solar cell (DSSC). *Energy Proc*. 2015;79:799–807.
71. Hossain M. a, Ngo HH, Guo WS, Nguyen TV, Vigneswaran S. Performance of cabbage and cauliflower wastes for heavy metals removal. *Desalin Water Treat*. 2013:1–17.
72. Beecher CWW. Cancer preventive properties of varieties of *Brassica oleracea*: a review. *Am J Clin Nutr*. 1994;59.

Manuscript received Mar. 25, 2017, and revision received Aug. 10, 2017.